

ISOLATING AND IDENTIFYING GENES OF INTEREST IN
THE BRUNNER'S GLAND

by

ALISON M. MONAHAN

A THESIS

Presented to the Department of Biology
and the Robert D. Clark Honors College
in partial fulfillment of the requirements for the degree of
Bachelor of Science

June 2018

An Abstract of the Thesis of

Alison M. Monahan for the degree of Bachelor of Science
in the Department of Biology to be taken June 2018

Title: Isolating and Identifying Genes of Interest in the Brunner's Gland

Approved: _____

Dr. Anne E. Zemper

The Brunner's Gland is a small comma-shaped gland, located at the gastrointestinal junction, that is responsible for neutralizing stomach acid and lubricating the intestinal walls. Previous research shows differences regarding the Brunner's Gland and the intestinal epithelium on the protein level. Yet, until this point, no research has been done to identify specific gene expression within the Brunner's Gland.

Within my research, I ask the question: what gene expression is unique to the Brunner's Gland? Through previous research regarding the functional and morphological comparison of the Brunner's Gland to the surrounding intestinal epithelium, I hypothesize there are certain genes differentially expressed within the Brunner's gland, in comparison to the surrounding intestinal epithelium, that are necessary for the homeostatic function of the Brunner's Gland.

To compare the gene expression profile of the Brunner's Gland to the overlying intestinal epithelium, Quantitative Real Time Polymerase Chain Reaction (qRT-PCR) is utilized. A sampling of relevant genes was chosen for the qRT-PCR process to distinguish the Brunner's Gland from the intestinal epithelium. A wildtype murine

model was used to analyze gene expression of the Brunner's Gland. After Brunner's Gland and surrounding epithelial tissue were isolated, mRNA was extracted, and cDNA synthesized for gene expression analysis.

The genetic profile of the Brunner's Gland will help generate more hypotheses and contribute to further research regarding how specific genes influence the development and function of the normal gland. As the Brunner's gland has been shown to be involved with Celiac disease and intestinal cancers, a gene expression profile for the Brunner's Gland will add to our knowledge of a healthy gland, and thus how to restore homeostasis in disease states.

Acknowledgements

To begin, I want to thank my primary thesis advisor and mentor, Dr. Annie Zemper, for supporting me throughout my undergraduate career. I want to thank her for answering all of my questions throughout the research and writing process, as well as knowing when to encourage me to search for the answer on my own. She has taught me how to be an intelligent, independent woman who can not only have a rewarding academic career, but also a fulfilling personal life.

Many thanks to the other members of my thesis committee: Dr. Kryn Stankunas, Dr. Melissa Grayboyes, and Professor Cristin Hulslander. Thank you for taking time out of your busy schedules to assist in the completion and defense of my thesis.

To the other members of the Zemper Lab, thank you for your sustained encouragement. Natalie—thank you for being my biggest cheerleader throughout this process. I will never be able to thank you enough for the advice and support you gave me during a very stressful time. Janelle—thank you for always reminding me to take a deep breath. Tim—thank you for dedicating time out of your busy life to help me interpret and analyze seemingly endless files of data.

Most importantly, I want to thank all of my friends and family who have stuck by my side during my rigorous academic career and the daunting task of writing an honors undergraduate thesis. I want to thank my mom and dad for never letting me forget that I can do anything with a lot of hard work, determination, patience, and a smidge of humor.

Table of Contents

Introduction	1
Background	2
Research Question and Hypothesis	10
Methods & Materials	12
Choice of Murine Model Organism	12
Isolation of Brunner's Gland and Small Intestinal Cells	12
mRNA Isolation	14
Reverse Transcription of mRNA to cDNA	15
Selection of qRT-PCR Primers	15
qRT-PCR	18
Statistical Analysis	21
Results	22
Discussion	25
Glossary	30
Bibliography	32

List of Figures

Figure 1: Diagram of the gastrointestinal system with the lining of the small intestine magnified.	1
Figure 2: Wild-type murine Brunner's Gland stained with Hematoxylin and Eosin.	3
Figure 3: Lineage allocation pathway of intestinal stem cells.	6
Figure 4: Morphology comparison of wild-type Brunner's Gland and Spdef-null Brunner's Gland.	8
Figure 5: Adult Brunner's Gland antibody stains for Aqp5, Muc6, and ErbB2 in wild-type and Spdef-null mice.	9
Figure 6: Wild-type Brunner's Gland antibody stains for Aqp5 at various murine developmental stages.	10
Figure 7: Stains of dissected and isolated Brunner's Gland with DAPI and AQP5.	14
Figure 8: <i>Actin</i> melt curves at 62 °C.	19
Figure 9: <i>Spdef</i> melt curves at 58 °C.	20
Figure 10: Box and whisker plots for the relative expression of various genes of interest in the Brunner's Gland compared to the small intestinal epithelium.	23

List of Tables

Table 1: qRT-PCR primers used for gene expression analysis.	17
Table 2: p-values for the relative expression of Brunner's Gland sample compared to normalized epithelium sample.	24

Introduction

The small intestine is made up of three sections respectively identified as the duodenum, jejunum, and ileum. The small intestine is a tube of smooth muscle between the stomach and the large intestine that is predominantly responsible for the absorption of nutrients from digested food into the bloodstream. The absorption of nutrients is facilitated through microscopic “finger-like” projections called villi along the intestinal wall (Wood and Montgomery 2014). A diagram of the small intestinal lining is presented in Figure 1 alongside an anatomical layout of the gastrointestinal system.

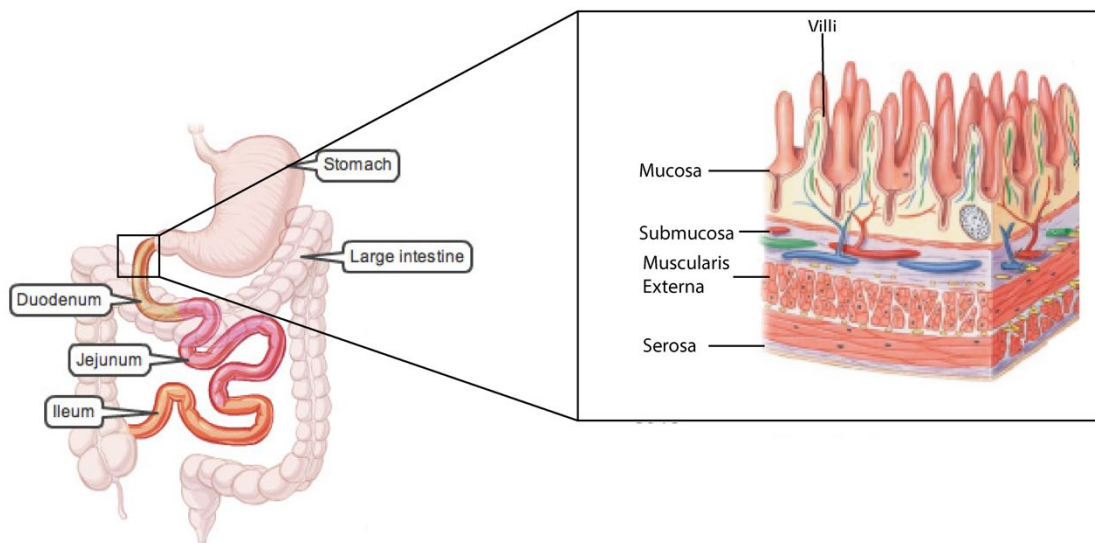


Figure 1: Diagram of the gastrointestinal system with the lining of the small intestine magnified.

This simple diagram of the gastrointestinal system shows the three sections of the small intestine: duodenum, jejunum, and ileum. The magnified inset displays the intestinal villi situated above the submucosal layer of the small intestine, which is where the Brunner’s Gland is located.

The Zemper Lab in the Institute of Molecular Biology at the University of Oregon focuses on research regarding cell differentiation and development in the small

and large intestine of a murine (mouse) model. Specifically, research in this lab attempts to uncover the complexities of stem cell origination, differentiation, and migration in the crypts of the intestinal epithelium. The research aims to yield a greater scientific understanding of the molecular and cellular mechanisms responsible for healthy (homeostasis) and disease states in the intestinal tract. This research is significant because an understanding of normal cellular processes in the intestinal system provides insight into how intestinal diseases such as ulcerative colitis, Celiac disease, and cancer develop in humans.

My current research focuses primarily on the characterization of genes in the Brunner's Gland—a small intestinal gland that is responsible for neutralizing stomach acid and lubricating the intestinal walls. The genetic profile of the Brunner's Gland has yet to be thoroughly characterized. I will distinguish the gene expression of the Brunner's Gland from the overlying small intestinal epithelium. The Brunner's Gland plays a crucial role in the healthy function of the small intestine; thus, researchers must determine the gene expression of the Brunner's Gland in homeostasis to understand the manifestation of disease linked to a dysfunctional Brunner's Gland in the small intestine.

Background

Brunner's Gland Morphology and Function

In mice, the Brunner's Gland is a small comma-shaped gland near the gastrointestinal junction as seen in Figure 2.

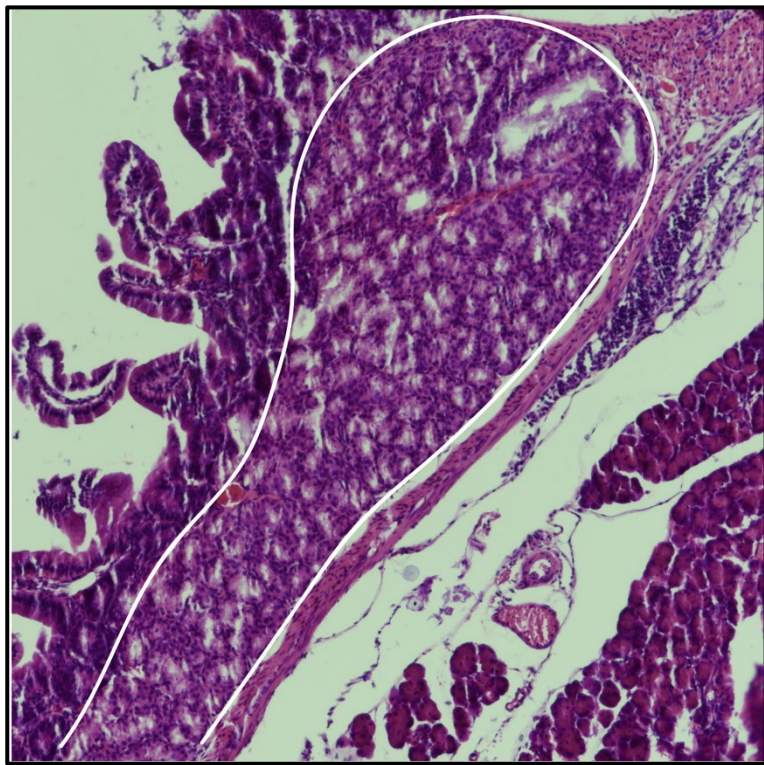


Figure 2: Wild-type murine Brunner's Gland stained with Hematoxylin and Eosin.

A wild-type murine Brunner's Gland is stained with Hematoxylin and Eosin—a stain that marks the cell nuclei and cellular structures within tissue samples. The comma-shaped gland is outlined in white (Parappilly et al., *in preparation*).

More specifically, the Brunner's Gland is located within the submucosal layer at the proximal end of the small intestinal duodenum. Previous research demonstrates that the Brunner's Gland develops postnatally within the sub-mucosal layer of the small intestine (Obuoforibo and Martin, 1977). As a secretory gland, the Brunner's gland secretes an alkaline-rich mucus into the small intestine to neutralize stomach acid (Collaco et al. 2013). The alkaline-rich secretions contain sodium bicarbonate and other mucins that aide in the protection and lubrication of the small intestinal wall (Collaco et al. 2013). These mucins are thought to act as a physical and chemical barrier to threats such as enteric bacteria and environmental toxins (Specian and Oliver 1991). Without

the secretory function of the Brunner's Gland, the intestinal wall would be susceptible to extreme damage and ulceration from the small amounts of acidic chyme released from the stomach during digestion. A healthy, non-ulcerated small intestine is important for the effective absorption of nutrients into the bloodstream.

Dysfunctional Brunner's Gland and Disease States

While tumors of the Brunner's Gland are rare, previous pathology reports have identified adenomas of the Brunner's Gland in humans (Gao et al. 2004). Most tumors of the Brunner's Gland are asymptomatic, yet a small portion of symptomatic tumors can result in intestinal obstruction and hemorrhage (Gao et al. 2004). One possible reason for the development of these tumors is a concurrent infection with *Helicobacter pylori* (*H. pylori*) (Kovacević et al. 2001). The *H. pylori* bacteria is responsible for chronic inflammation of the small intestine and the subsequent increased occurrence of intestinal diseases and cancers (Wroblewski et al. 2010). *H. pylori* is a type I carcinogen that can easily colonize harsh environments such as the acidic chyme of the stomach (Wroblewski et al. 2010). According to Kovacević and colleagues, 71% of patients diagnosed with an adenoma of the Brunner's Gland had a concurrent *H. pylori* infection at the time of diagnosis (Kovacević et al. 2001). Further research into the development, structure, and function of the Brunner's Gland will aide in a better understanding of the development of disease states alongside a *H. pylori* infection.

Celiac disease, a chronic inflammatory disorder of the small bowel, is a common ailment that negatively impacts the gastrointestinal system. The disorder is commonly associated with increased inflammation in the duodenum that results in malabsorption and diarrhea in affected individuals (Collaco et al. 2013). Recently, researchers have

noticed a reduced presence of transporter proteins, such as Aqp5, within the Brunner's Glands of active Celiac patients (Collaco et al. 2013). A reduced presence of transporter proteins could be linked to the loss of absorptive function and subsequent chronic diarrhea within Celiac patients. Still, there is much to learn in regard to the connection between Celiac disease and a dysfunctional Brunner's Gland. An initial investigation into the expression of *Aqp5* in a healthy gland could contribute to understanding the gland in homeostasis. Then, researchers could further research the manifestation of disease within the small intestine by looking at how a lack of *Aqp5* expression in the Brunner's Gland disrupts intestinal homeostasis.

Cell Differentiation in the Brunner's Gland

The Zemper Lab has previously focused on the role of specific proteins in the structural and functional development of the Brunner's Gland. To try to understand Brunner's Gland secretory cell development, we have tried to place the Brunner's Gland within the paradigm of the generation of secretory cells in the neighboring intestinal tissue. To summarize, the stem cells at the bottom of the small intestinal crypts replace old cells and differentiate into a variety of different cell types depending on the needs of the small intestine, which include the replenishment of epithelial cells to maintain a healthy intestinal lining and the secretion of mucus-based substances to lubricate the epithelial walls. The process of cell differentiation within the crypts is facilitated by a variety of proteins that participate in the signaling pathway as seen below in Figure 3.

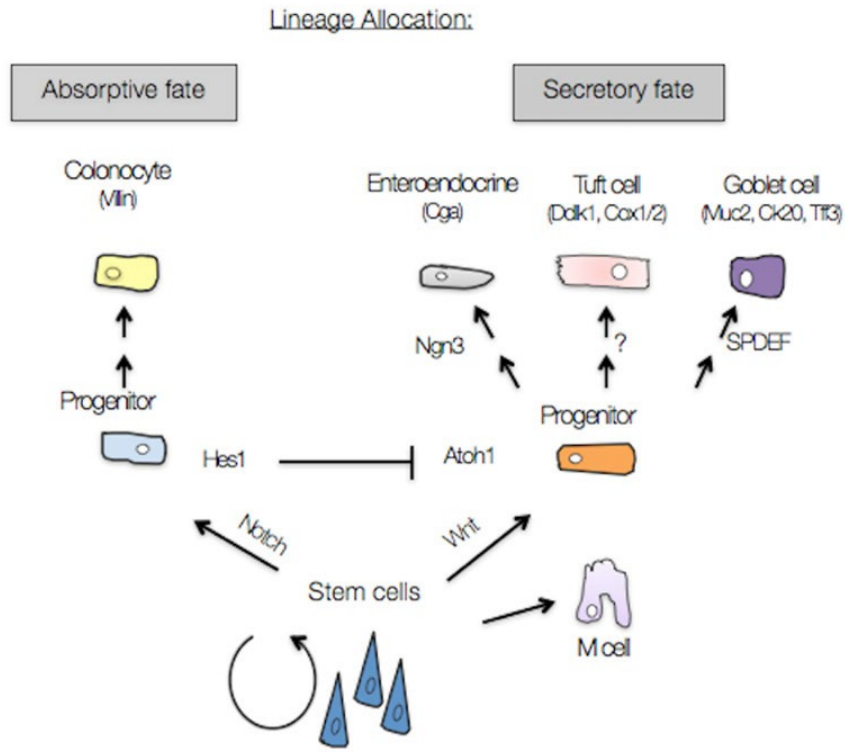


Figure 3: Lineage allocation pathway of intestinal stem cells.

The lineage allocation pathway of intestinal stem cells illustrates cell differentiation along the Notch pathway into an absorptive fate or along the Wnt pathway into a secretory fate. The Brunner's Gland follows a secretory pathway similar to goblet cells (Zemper Lab).

Some cells differentiate into secretory cells, similar to the ones found in the Brunner's Gland, while other cells can differentiate into absorptive cells, such as the ones found throughout the epithelium of the small intestine. The Notch protein signals intestinal stem cells to turn into absorptive progenitor cells, while the Wnt protein signals intestinal stem cells to turn into secretory progenitor cells. Goblet cells, from the secretory cell fate, are similar to Brunner's Gland cells due to their shared function of the secretion of mucins (Specian and Oliver 1991). The role of proteins and cell differentiation has assisted in elucidating the secretory function of the Brunner's Gland,

yet information on the genetic background of the Brunner's Gland will further add to our knowledge regarding the gland's function.

Development of the Brunner's Gland

Previous research within the Zemper Lab built a more complete understanding of the development of the Brunner's Gland on a molecular level. From that research we know that Brunner's Gland cells arise from Lrig1-expressing cells instead of Villin-expressing cells; and due to the fact that Villin is commonly found in the intestinal epithelium, the gland is proposed to be of more gastric origin (Parappilly 2016). The Zemper lab also discovered that Spdef was a crucial protein for Brunner's Gland development. Adult Spdef null mice had largely underdeveloped and deformed Brunner's Glands as shown in Figure 4.

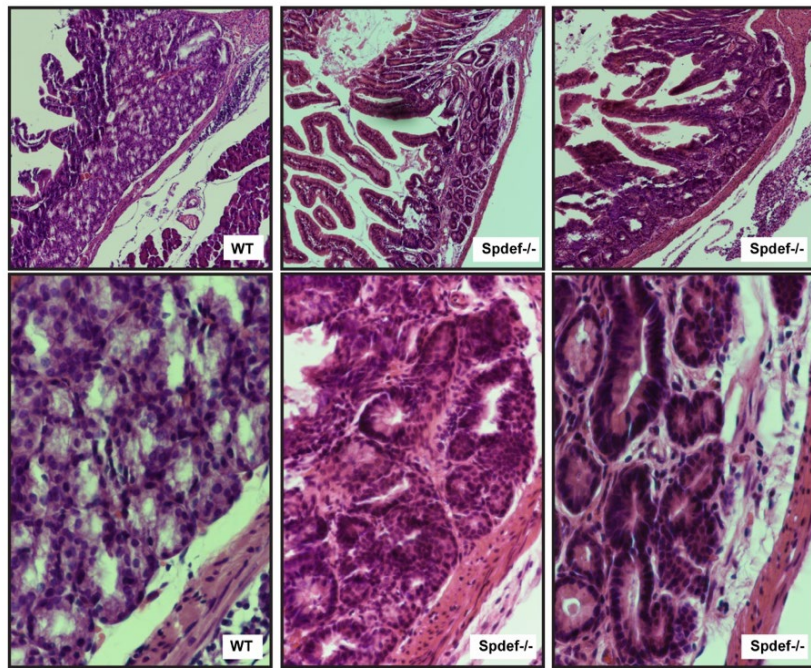


Figure 4: Morphology comparison of wild-type Brunner's Gland and Spdef-null Brunner's Gland.

The Spdef-null Brunner's Gland within the adult mouse shows drastic morphological differences in comparison to the wild-type Brunner's Gland. The glandular structures with the Spdef-null mice are noticeably deformed, and even the gland itself appears physically smaller (Parappilly 2016).

After determining the importance of Spdef in the development of the Brunner's Gland, researchers looked into the differences in protein expression between wild-type and Spdef-null adult murine glands through the use of antibody stains for proteins such as Aqp5, ErbB2, and Muc6. While expression of the ErbB2 and Muc6 antibodies did not differ between wild-type and Spdef-null animals, expression of the Aqp5 antibody was lost in Spdef-null mice compared to wild-type mice (Parappilly 2016, Figure 5).

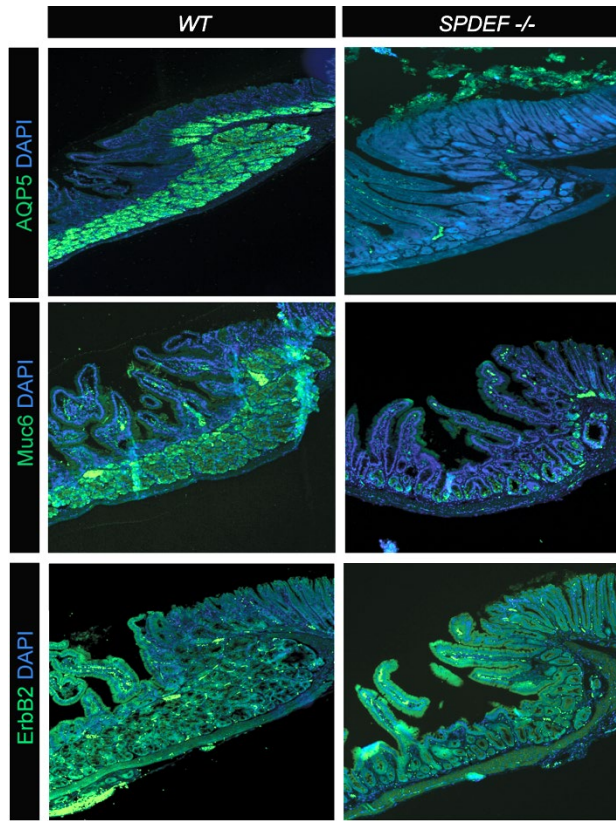


Figure 5: Adult Brunner's Gland antibody stains for Aqp5, Muc6, and ErbB2 in wild-type and Spdef-null mice.

The stains for Aqp5, Muc6 and ErbB2 are expressed in green. The blue stain is DAPI which binds to all cell nuclei, providing greater visualization of cell shape and size. Spdef-null mice display wild-type expression of ErbB2 and Muc6, while Spdef-null mice lack normal Aqp5 expression (Parappilly et al., in preparation).

These findings suggest that Aqp5 is impeded by the loss of Spdef, yet Muc6 and ErbB2 are still expressed in the Brunner's Gland in the absence of Spdef (Parappilly 2016). In addition, the murine Brunner's Gland presenting Aqp5 expression can be seen as early as post-natal day five in mice (Marin 2017, Figure 6).

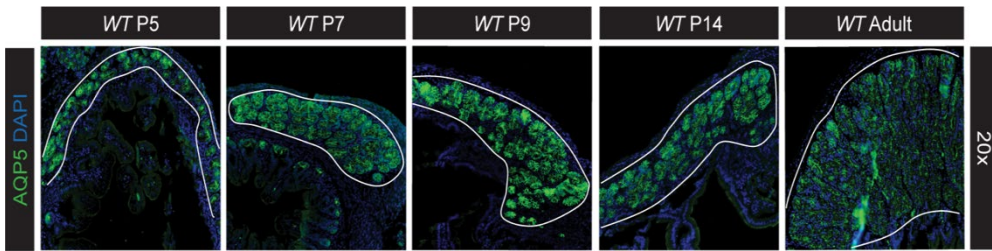


Figure 6: Wild-type Brunner's Gland antibody stains for Aqp5 at various murine developmental stages.

The development of the Brunner's Gland and the presence of Aqp5 develop simultaneously, seen as early as post-natal day five in a wild-type mouse. The stain for Aqp5 is expressed in green and the blue stain is DAPI (Parappilly et al., in preparation).

The observations made within previous research on the Brunner's Gland can help narrow down a potential list of genes for the genetic profiling of a wild-type Brunner's Gland. Due to the critical involvement of Spdef and Aqp5 in the development of the Brunner's Gland, these proteins will be analyzed on the level of gene expression. The Brunner's Gland secretes mucins to maintain a healthy intestinal epithelium, and as a result, the gene expression of various mucins will also be analyzed within a wild-type gland. Various other genes associated with cell differentiation and stem-cell origination will also be analyzed within the Brunner's Gland.

Research Question and Hypothesis

For my research, I want to ask a simple, yet crucial question: what gene expression is unique to the Brunner's Gland? Through previous research regarding the functional and morphological comparison of the Brunner's Gland to the surrounding intestinal epithelium, I hypothesize there are certain genes differentially expressed within the Brunner's gland, in comparison to the surrounding intestinal epithelium, that are necessary for the homeostatic function of the Brunner's Gland.

As a first step in testing this hypothesis, I will compare the gene expression profile of cells from the Brunner's Gland to that of the overlying intestinal epithelium, through a gene expression profiling process known as Quantitative Real-Time Polymerase Chain Reaction (qRT-PCR).

Methods & Materials

Choice of Murine Model Organism

The Brunner's Gland is specific to mammalian species including humans and mice. I utilized the laboratory mouse, or *Mus musculus*, as a model to better understand gene expression surrounding the function and morphology of the Brunner's Gland. The *Mus musculus* is a convenient and advantageous model organism in my research because they reproduce and mature quickly for efficient harvest of the Brunner's Gland from wild-type adult mice. The Brunner's Gland of the mouse is a compact organ of about 2 to 5 mm in length (Obuforibo and Martin 1977); and as a result, can easily be isolated within a specific region of the small intestine. Furthermore, mice are genetically similar to humans, which allows for viable comparison of the gland's morphology and function between mice and humans. If we can understand the genetic complexity behind the murine Brunner's Gland, we can better understand disease development and progression due to a dysfunctional Brunner's Gland in humans. A total of eighteen mice were sacrificed within this sampling. The mice used in these experiments ranged in age from six to ten weeks.

Isolation of Brunner's Gland and Small Intestinal Cells

To begin, small intestinal epithelium cells were isolated from a sample size of three mice. Thus, each biological replicate within a qRT-PCR run included three mice. Once the mice were sacrificed under Animal Care Services (ACS) regulations, a section of the small intestine, including the Brunner's Gland at the gastrointestinal junction, was dissected out. Any excess fat and mesentery was removed, and the tissue was

flushed with phosphate-buffered saline (PBS). The pieces of murine small intestine were then placed in 20 mL of a solution of 30 uL of 30 mM EDTA and 20 mL of 1.5 mM DTT, and rocked at 4 °C. The rocking of the tissue in the dissociation reagent allows for more effective removal of the intestinal crypts from the small intestinal wall. After forty minutes, the tissue was transferred into 20 mL of 30 mM EDTA and rocked at room temperature for eight minutes. The tube was then physically shaken to separate the intestinal epithelium cells from the tissue sample. The intestinal pieces were then transferred to another 20 mL of 30mM EDTA and placed in a 37 °C water bath for three minutes. The tube was shaken once more, and the remaining intestinal pieces were removed and placed in a wax tray filled with PBS. The remaining mixture of epithelial cells and 30 mM EDTA were centrifuged to pellet the small intestinal epithelial cells. The supernatant (liquid above the pellet) was poured off and the remaining pellet at the bottom of the tube was flash-frozen in liquid nitrogen.

The remaining pieces of small intestine were dissected underneath a KL 1500 LED dissecting microscope with the mesenchymal side up. The muscle layer of the small intestine was removed to access the Brunner's Gland. Using forceps, the Brunner's gland tissue was removed and placed in a sample collection tube and flash frozen in liquid nitrogen. In Figure 7, the remaining piece of small intestine, including any leftover Brunner's Gland, and the isolated portion of Brunner's Gland were fixed and stained in order to confirm isolation of Brunner's Gland tissue.

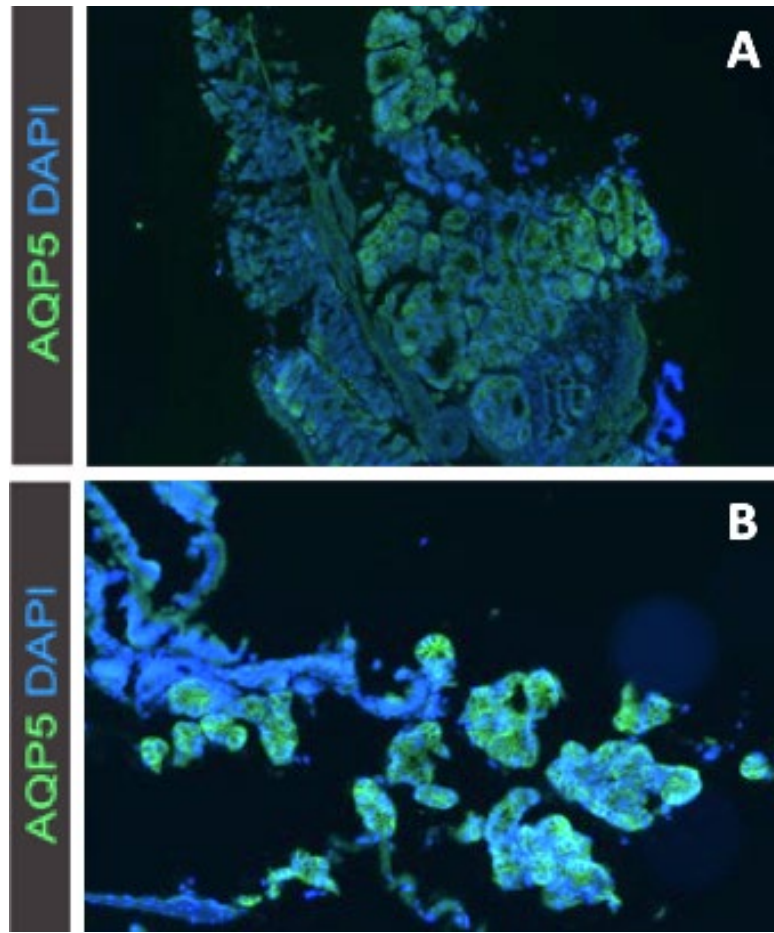


Figure 7: Stains of dissected and isolated Brunner's Gland with DAPI and AQP5.

After an isolation protocol, the remaining piece of small intestine (top) and the isolated Brunner's gland tissue (bottom) were stained with DAPI and AQP5. DAPI presents as a bright blue stain, while AQP5 presents as a green stain. Figure 7A indicates the Brunner's gland in which the tissue was scraped away. The isolated tissue is shown in the Figure 7B (Zemper Lab, unpublished).

mRNA Isolation

The mRNA isolation of the small intestinal epithelium and the Brunner's Gland cell samples was performed with the RNA Mini Kit from *Qiagen*. In short, the cells were lysed, and mRNA was extracted through a series of solution washes and extractions. During this procedure, resident genomic DNA from the cells was degraded using DNase. The concentration of mRNA within both the intestinal epithelium and

Brunner's gland samples was measured on a spectrophotometer in order to determine the concentration of isolated mRNA, as a precursor to reverse transcription of cDNA.

Reverse Transcription of mRNA to cDNA

The synthesis of cDNA is done through a protocol developed by *Thermo Scientific* for first strand cDNA synthesis. An oligo (dT)₁₈ primer is used specifically for the synthesis. The cDNA is reverse transcribed from mRNA using a reverse transcriptase enzyme. The negative control is a sample without the addition of the reverse transcriptase enzyme. The absence of genomic DNA was confirmed through general polymerase chain reaction (PCR) and agarose gel electrophoresis. Samples with the addition of reverse transcriptase should amplify for actin within the general PCR reaction, while there should be no amplification in the negative controls. The cDNA concentrations were measured on a spectrophotometer to ensure a sufficient amount of cDNA for qRT-PCR.

Selection of qRT-PCR Primers

When selecting primers for each gene of interest, multiple criteria were taken into account. Primer sequences should have a GC content around 50-60% and be approximately 18-28 nucleotide bases in length. These parameters ensure maximum product stability and efficiency within the reaction. The forward and reverse primer sequences of each gene should also avoid complementarity in order to prevent the formation of primer dimers. Furthermore, forward and reverse primers should have compatible melting temperatures, or T_m values, so as to make certain that there is a smaller likelihood of partially melted amplicons or amplification of off-target amplicons

within the reaction. All of the potential primer sequences were run against genomic-wide BLAST searches in order to confirm that the sequences were located with exons, not introns. This distinction is necessary because the cDNA used in the qRT-PCR reactions has been reverse transcribed from mRNA, which does not include introns.

All primers were ordered according to the desalting specifications for qRT-PCR through Sigma-Aldrich. Primer sequences were obtained one of three ways: previously used sequences within the Zemper Lab, review of current literature involving qRT-PCR, or predesigned KiCqStart SYBR Green Primers through Sigma-Aldrich. Primer sequences from the Zemper Lab included *Lgr5*, *Villin*, *Muc2*, *Egfr*, *Tgfa*, and *Actin*. KiCqStart SYBR Green Primers included *ErbB2*, *Aqp5*, and *Bmi-1*. Primers from review of current literature included *Spdef* and *Muc6* (Horst et al. 2010). Table 1 includes genes, forward and reverse primer sequences, and annealing temperatures.

Gene	Primer Sequences	Annealing Temp. (°C)
<i>Actin</i>	F: 5'-TACCACCATGTACCCAGGCA-3' R: 5'-CTCAGGAGGAGCAATGATCTTGAT-3'	62
<i>Lgr5</i>	F: 5'-GGAAGCGCTACAGAATTGA-3' R: 5'-AGGCGTAGTCTGCTATGTGG-3'	57
<i>Villin</i>	F: 5'-GATCTCCCAGGTGGTGGCTGC-3' R: 5'-CGGGAGTGGTGATGTTGAGAGAGC-3'	62
<i>Muc2</i>	F: 5'-GGTCCAGGGTCTGGATCACA-3' R: 5'-GCTCAGCTCACTGCCATCTG-3'	62
<i>Egfr</i>	F: 5'-GTGATGGGGATGTGATCATT-3' R: 5'-AGCATAAAGGATTGCAGACG-3'	58
<i>Tgfa</i>	F: 5'-CACTGGACTTCAGCCCTCTA-3' R: 5'-TCCAGCAGACCAGAAAAAGAC-3'	57
<i>ErbB2</i>	F: 5'-GCTTTGAGGACAAGTATG-3' R: 5'-AAGATCTCTGTGAGACTTCG-3'	57
<i>Aqp5</i>	F: 5'-GGAGTTAACCTGACTTCCAG-3' R: 5'-AAGTAGATCCCCACAAGATG-3'	53
<i>Bmi-1</i>	F: 5'-GGAAGAGGTGAATGATAAAAGG R: 5'-CATGACGTCAATCAAATCTGGAAAG-3'	57
<i>Spdef</i>	F: 5'-TTGGATGAGCACTCGCTAGA-3' R: 5'-AGCCGGTACTGGTGTCTGT-3'	58
<i>Muc6</i>	F: 5'-CTCCTCACCTCTACCCCAGT-3' R: 5'-TCTGGTGCTCTCCTCCTGT-3'	58

Table 1: qRT-PCR primers used for gene expression analysis.

Forward and reverse primer sequences were identified through resources within the Zemper Lab, review of current literature, and predesigned KiCqStart sequences from Sigma-Aldrich. The documented annealing temperatures were the values in which the primers were run for gene expression analysis of the Brunner's Gland compared to the intestinal epithelium.

qRT-PCR

The cDNA was diluted to 100 ng/uL with RNase-free water. A master mix for the qRT-PCR reaction included SYBR-green FAST super mix, which contains a fluorescent DNA-binding dye, and water with both reverse and forward DNA primers. The wells with only master mix are a negative control for the process, while the wells with cDNA and master mix help determine gene expression levels within the Brunner's Gland compared to the small intestinal epithelium. Once 18 uL of master mix and 2 uL of cDNA had been distributed in each well, a 96-well plate was placed in the 0.1 mL block of the Thermo Fisher QuantStudio 3 machine. Through fluorescent markers in the SYBR-green FAST super mix, the amplified DNA was marked in real-time as the DNA replication cycles occurred. The frequency of fluorescent markers can determine the relative levels of gene expression in the Brunner's gland compared to the intestinal epithelium.

Primer Sequence Verification and Optimization

Each potential primer sequence was verified and optimized for the Thermo Fisher QuantStudio 3 machine. By using the melting temperature (T_m) of each primer, which was on the technical datasheets provided by Sigma Aldrich, the annealing temperature was calculated by subtracting 5 °C from the provided T_m value. Samples of small intestinal cDNA were used to verify and optimize qRT-PCR conditions for each primer; while water was the designated negative control.

Accurate gene expression analysis depends on amplification of a pure and specific target sequence. The melting characteristics of each primer set were assessed by looking at the post-amplification melt curve, or dissociation curve. When run at the

optimal annealing temperatures, an optimal primer set that produces a single product is distinguished by a singular, distinct peak on a plot for $-\Delta F/\Delta T$ (change in fluorescence/change in temperature) versus temperature. Melt curves for *Actin* and *Spdef* are displayed in Figure 8 and 9 respectively. In addition, an efficient primer set is designated by a doubling of amplification products every cycle; and this trend can be observed through qRT-PCR amplification curves performed in a basic thermal cycling program.

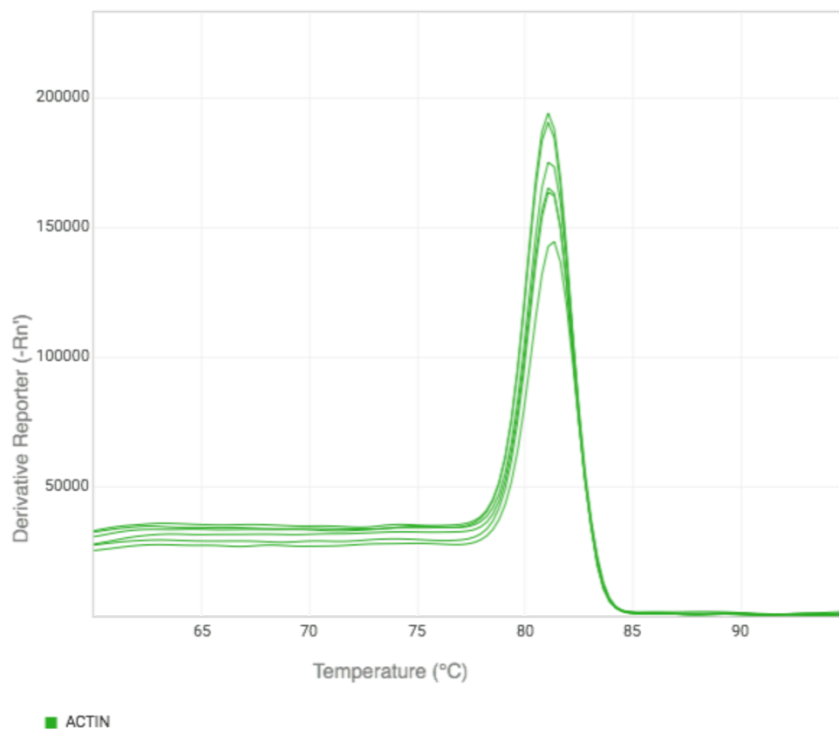


Figure 8: *Actin* melt curves at 62 °C.

The primer set for *Actin* is verified and optimized through a basic melt curve analysis following the typical thermal cycling program on the qRT-PCR machine. A distinct, singular peak along the curve indicates primer specificity and efficiency.

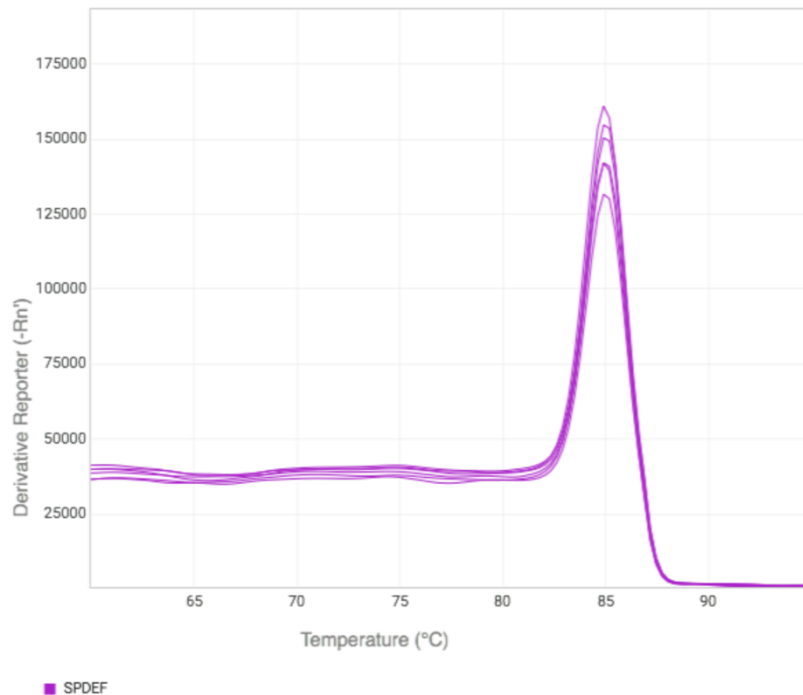


Figure 9: *Spdef* melt curves at 58 °C.

The primer set for *Spdef* is verified and optimized through a basic melt curve analysis following the typical thermal cycling program on the qRT-PCR machine. A distinct, singular peak along the curve indicates primer specificity and efficiency.

Gene Expression Analysis

A 96-well format with veriflex optimization was utilized during each comparative C_T experimental run. A total of ten genes of interest were analyzed and compared against an endogenous control gene, *Actin*. Intestinal epithelium cDNA was the reference sample and Brunner's Gland cDNA was the target sample. Water was once again used as the negative control. Overall, each gene of interest was run in triplicate across six biological replicates.

Statistical Analysis

The generation of qRT-PCR results were obtained through the ThermoFisher Connect Relative Quantification application. All statistical analysis was performed on R-Studio with assistance from a graduate student in the Zemper Lab, Tim Wheeler. The test type used to analyze the results was a student's t-test for a two-tailed, paired sample. The test group was Brunner's Gland-derived sample and the control group was small intestinal epithelium-derived sample. The data was first normalized by mean actin response per gene per 96-well plate; and then by mean control group gene expression per plate.

Results

In order to analyze gene expression levels within the Brunner's Gland compared to the small intestinal epithelium, the relative quantity (RQ) values must be calculated. The equation for RQ is $2^{-\Delta\Delta CT}$. The RQ values were obtained by utilizing the cycle threshold values for each gene. The cycle threshold (C_t) value is the cycle number at which the sample fluorescence exceeds a set threshold for the background fluorescence (Bustin 2005). A large C_t value corresponds to less mRNA; while a small C_t value corresponds to a larger presence of mRNA. The raw C_t values were integrated into the $\Delta\Delta CT$ equation to solve for RQ, or relative fold change expression. All RQ values were calculated through the ThermoFisher Connect Relative Quantification application. The RQ of epithelium was set to a value of one to ensure that the data for gene expression in the Brunner's Gland was compared to normalized expression within epithelium cells.

We wanted to determine what genes were differentially expressed within the Brunner's Gland compared to the intestinal epithelium. A RQ value greater than 2 denotes a biologically relevant increase in gene expression compared to the reference sample. A RQ value less than 0.5 denotes a biologically relevant decrease in gene expression compared to the reference sample. A range of RQ values for each gene of interest follows: *Aqp5*: 16.602 to 1126.3; *Bmi-1*: 7.261 to 13.84; *Muc2*: 0.021 to 0.138; *Muc6*: 91.313 to 4230.6; *Egfr*: 0.319 to 1.22; *Spdef*: 7.946 to 225.9; *Villin*: 0.322 to 2.77; *Lgr5*: 0.82 to 6.1; and *ErbB2*: 1.631 to 4.246. The gene expression levels, or RQ values, for all genes of interest are displayed on the box and whisker plots shown below (Figure 10).

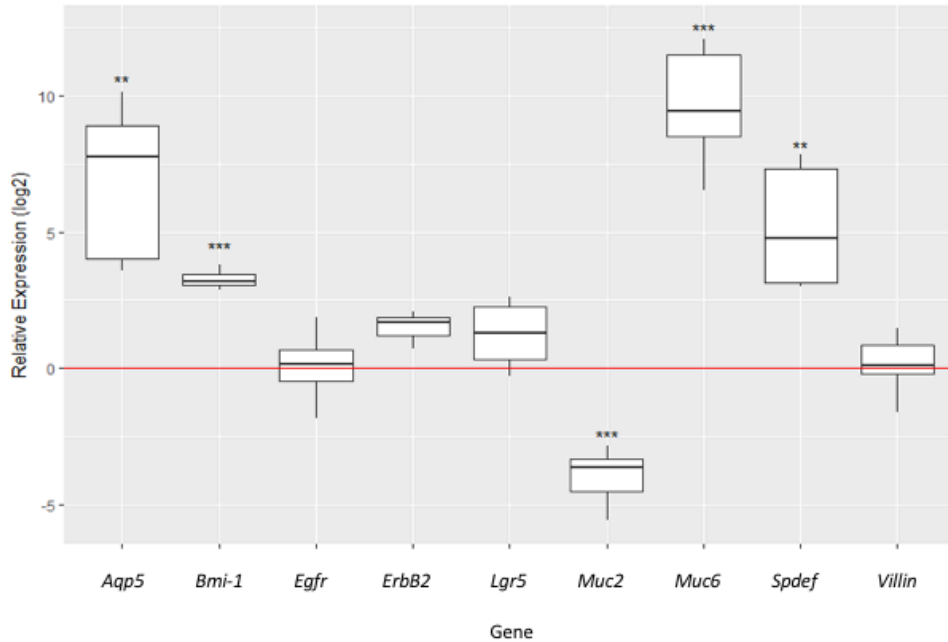


Figure 10: Box and whisker plots for the relative expression of various genes of interest in the Brunner's Gland compared to the small intestinal epithelium.

The RQ values, or fold change difference, across the six biological replicates are displayed through a standard box and whisker plot. The centerline for each plot is the median RQ value with the box extending from the 25th to the 75th percentile. The whiskers encompass 95% of the total confidence interval. The red line denotes baseline epithelial expression level. p-values were determined with a two-tailed, paired sample student t-test. Note: * p-value < 0.05; ** p-value < 0.01; and *** p-value < 0.001.

The highly expressed genes were *Aqp5*, *Bmi-1*, *Spdef*, and *Muc6*. *Muc2*, in contrast, was lowly expressed. The genes that did not show a biologically significant change in expression levels were *Egfr*, *Villin*, *ErbB2*, and *Lgr5*. *Tgfa* did not amplify consistently across Brunner's Gland samples; and as a result, RQ values for *Tgfa* could not be determined. The p-values for each gene are represented in Table 2.

Gene	p-value
<i>Aqp5</i>	0.00644
<i>Bmi-1</i>	0.00003
<i>Egfr</i>	0.92368
<i>ErbB2</i>	0.06801
<i>Lgr5</i>	0.16607
<i>Muc2</i>	0.00021
<i>Muc6</i>	0.00011
<i>Spdef</i>	0.00682
<i>Villin</i>	0.77281

Table 2: p-values for the relative expression of Brunner's Gland sample compared to normalized epithelium sample.

p-values were determined with a two-tailed, paired sample student t-test.

Discussion

Multiple genes within Brunner's Gland tissue displayed significantly different expression levels compared to the overlying intestinal epithelium. *Aqp5* is highly expressed in Brunner's Gland tissue compared to the small intestinal epithelium. *Aqp5* encodes for a small plasma membrane protein that is primarily responsible for water transport across the plasma membrane (Collaco et al. 2013). Due to the secretory function of the Brunner's Gland and its ability to transport fluids and mucins into the luminal space, we would expect high expression of *Aqp5* in the gland. Furthermore, previous antibody stains have displayed noticeable *Aqp5* expression within the Brunner's Gland compared to the small intestinal epithelium (Parappilly 2016). A statistically significant RQ value for *Aqp5* within the gland demonstrates that the expression of *Aqp5* is more highly expressed in the gland compared to the overlying epithelium. Since previous research has begun to make connections with *Aqp5* and the physical manifestations of Celiac disease, the discovery that *Aqp5* is highly expressed in a healthy gland encourages further exploration into the relationship between lower *Aqp5* expression and the presence and severity of Celiac disease (Collaco et al. 2013).

Next, *Bmi-1*, an intestinal stem cell marker, is also highly expressed in Brunner's Gland tissue compared to the small intestinal epithelium. Interestingly, the Brunner's Gland has previously been shown to be in a differentiated state (Figure 3); yet, the gland shows a significant expression of a specific intestinal stem cell marker. This introduces the possibility that the Brunner's Gland tissue has regenerative properties or performs a high rate of cell cycling. In addition, *Bmi-1* is a member of the polycomb-group family of proteins and displays oncogenic properties (Wang et al.

2015). An overexpression of Bmi-1 has been associated with increased cell proliferation and invasion in tumors of gastric origin (Wang et al. 2015). An overexpression on *Bmi-1* in cancerous Brunner's Gland tissue compared to *Bmi-1* levels in healthy Brunner's Gland tissue could provide one explanation for the development of adenomas in the Brunner's Gland.

Additionally, *Muc6* is highly expressed in Brunner's Gland tissue compared to the small intestinal epithelium. *Muc6* is primarily found within the proximal region of the duodenum of the small intestine and its gel-forming properties contribute to the mucus-based secretions of the Brunner's Gland (Krause 2000). As the Brunner's Gland is at the proximal region of the duodenum and secretes mucins, it is reasonable to observe high *Muc6* gene expression levels within Brunner's Gland tissue. The Brunner's Gland secretes various mucin glycoproteins, including *Muc6*, in order to contribute to the mucosal lining of the small intestine and protect the delicate underlying epithelial tissue (Krause 2000). The high expression of *Muc6* in the Brunner's Gland and the protective role of mucins could further explain the development of adenomas of the Brunner's Gland alongside a concurrent *H. pylori* infection.

Next, *Spdef* is highly expressed in Brunner's Gland tissue compared to the small intestinal epithelium. *Spdef* has been found to sufficiently promote goblet cell differentiation along the Notch signaling pathway (Noah et al. 2010). In addition, previous work has shown that *Spdef* plays a vital role in the development of the Brunner's Gland (Parappilly 2016). With the shared mucus-secreting properties of goblet cells and the previously discovered involvement of *Spdef* in the gland's

development, it is logical to also record high levels of *Spdef* within the Brunner's Gland.

The last significant finding is that *Muc2* is lowly expressed in Brunner's Gland tissue compared to the small intestinal epithelium. *Muc2* is another member within the mucin family that functions to coat the epithelium with a protective gel-like substance (Johansson et al. 2008). Therefore, we would expect to also see that *Muc2* is prominently expressed in the Brunner's Gland when running a gene expression analysis; yet, *Muc2* expression is lower compared to the small intestinal epithelium. One hypothetical explanation for this observation could be that specific mucins could be delegated to certain portions of the gastrointestinal system in order to more effectively protect against external irritants unique to that section of the intestines, however we have not yet explored this possibility.

Of the genes analyzed, *Egfr*, *ErbB2*, *Lgr5*, and *Villin* did not have significant gene profiles between Brunner's gland and small intestinal epithelium, and as a result, definite conclusions cannot be made. *Egfr* and *Villin* qualitatively cluster around the set point for epithelium, while *ErbB2* and *Lgr5* hover slightly above the set point for epithelium. Qualitatively, all of these genes display similar gene expression profiles in the Brunner's Gland compared to the intestinal epithelium, yet we cannot make any definitive quantitative conclusions. Still, one discrepant observation is that the RQ values for *Villin* in the Brunner's Gland are extremely similar to the set-point of one for epithelium. We would expect to see lower expression of *Villin* in the Brunner's Gland because Brunner's Gland cells arise from Lrig1-expressing cells of gastric origin instead of Villin-expressing cells of intestinal origin (Parappilly 2016); yet *Villin* in the

Brunner's gland is qualitatively expressed at the same levels as the overlying epithelium. On the other hand, we must consider the fact that past lineage tracing experiments on the Brunner's Gland with Lrig1 and Villin were performed on mice at post-natal day one. While there is an absence of Villin-expressing cells in post-natal day one mice, Villin could begin to be expressed later on in glandular development. This occurrence later in development could account for the gene profile of *Villin* in the Brunner's Gland compared to the small intestinal epithelium. Further analysis needs to be done to address this discrepancy.

Across this gene expression analysis, RQ values varied dramatically, yet indicated a consistent trend in either higher or lower gene expression in the Brunner's Gland compared to the overlying small intestinal epithelium. While the data is consistent for trends in expression levels, the individual variability may be attributed to the macro-dissection of Brunner's Gland. While the method of isolation was previously verified with staining for Aqp5, this method primarily enriches for the glandular tissue, but it is not a pure method of isolation. Due to the macro-dissection, the sample may have included other cell types surrounding the gland, including smooth muscle cells, epithelial cells, and cells lining the end of the gastrointestinal junction. As these varying cell types have different gene expression, the method of isolation is not 100% pure, and thus the significance of individual values of relative expression must be considered with caution.

The Brunner's gland provides a crucial function in maintaining homeostasis within the digestive system. The Brunner's Gland protects the small intestinal epithelium from acidic ulceration by secreting alkaline-based substances, while

additionally lubricating the intestinal passageway to effectively facilitate nutrient absorption (Collaco et al. 2013). To better understand the Brunner's gland's role in homeostasis, and thus disease, this study focused on gene expression within the Brunner's Gland compared to the surrounding intestinal epithelium. The gene expression preliminarily measured will provide direction for future research regarding the significance of particular genes and their roles within the gland including: *Aqp5*, *Bmi-1*, *Muc6*, *Spdef*, *Muc2*, *ErbB2*, *Egfr*, *Villin*, and *Lgr5*.

My study illustrates the complexity of the Brunner's Gland. Certain genes are expressed at significantly different levels in the Brunner's Gland compared to the overlying small intestinal epithelium. The influence of these genes on the morphology and function of the gland needs to be further explored in order to better understand how the absence of certain genes affect the overall health of the gastrointestinal system. This research will aide in future studies that involve the development of disease in the gland and the surrounding small intestine.

Glossary

Adenoma: a benign tumor that originates from glandular structures within epithelial tissue

Annealing Temperature: the temperature at which two strands of denatured DNA rejoin and DNA returns to its natural state

Amplicon: a piece of DNA or RNA that is the source and/or product of an amplification event

Carcinogen: a cancer-causing agent

Chyme: a mixture of gastric secretions and partially digested food

Crypt: a valley-like structure between intestinal villi that are involved primarily with secretion of young epithelial cells from stem cells at its base

Differentiation: the process of one cell type changing into another cell type

Exon: a segment of DNA or RNA that encodes for a protein sequence

Gastrointestinal Junction: the place at which the stomach meets the small intestine

Gene: a sequence of DNA that codes for a specific function

Helicobacter pylori: a species of bacteria located in the stomach and intestine that is prone to causing ulcerations and cancer

Hemorrhage: an excessive amount of bleeding

Intron: a segment of DNA or RNA that does not encode for a protein sequence

Lysis: the breakdown of the cell membrane

Null: the result of a genetic technique in which a gene that encodes for a protein or enzyme is inactivated

Primer Dimer: an amplification product resulting from the interaction between the forward and reverse primer

Stem Cell: an undifferentiated cell type that can give rise to the same undifferentiated cell type or differentiate into a more specialized cell type

Transporter Protein: a type of protein used in the movement of ions and molecules across a biological membrane

Ulceration: the disintegration of epithelial tissue due to a breach in skin or mucous membranes

Ulcerative Colitis: a disease of the large intestine that results in chronic inflammation and ulceration of the mucosal wall

Veriflex: a temperature control technology that allows designation of up to three different temperature zones on the qRT-PCR block

Wild-Type: the standard, non-mutated version of a gene

Bibliography

- Collaco AM, Jakab RL, Hoekstra NE, Mitchell KA, Brooks A, Ameen NA. 2013. Regulated traffic of anion transporters in mammalian Brunner's glands: a role for water and fluid transport. *Am. J. Physiol. Gastrointest. Liver Physiol.* 305: G258-75.
- Bustin SA, Benes V, Nolan T, Pfaffl MW. 2005. REVIEW Quantitative real-time RT-PCR – a perspective. *J. Mol. Endocrinol.* 34:597–601.
- Gao Y-P, Zhu J-S, Zheng W-J. 2004. Brunner's gland adenoma of duodenum: A case report and literature review. *World J Gastroenterol World J. Gastroenterol. World J Gastroenterol* 10: 2616–2617.
- Horst D, Gu X, Bhasin M, Yang Q, Verzi M, Lin D, Joseph M, Zhang X, Chen W, Li Y-P, et al. 2010. Requirement of the epithelium-specific Ets transcription factor Spdef for mucous gland cell function in the gastric antrum. *J. Biol. Chem.* 285:35047–55.
- Johansson ME V, Phillipson M, Petersson J, Velcich A, Holm L, Hansson GC, Greenberg EP. 2008. The inner of the two Muc2 mucin-dependent mucus layers in colon is devoid of bacteria. *PNAS* 105 (39): 15064-15064.
- Kovacević I, Ljubicić N, Cupić H, Doko M, Zovak M, Troškot B, Kujundžić M, Banić M. 2001. Helicobacter pylori infection in patients with Brunner's gland adenoma. *Acta Med. Croatica* 55:157–60.
- Krause, WJ. Brunner's glands: a structural, histochemical and pathological profile. *Progress in histochemistry and cytochemistry* 35.4 (2000): 255-367.
- Marin M. 2017. Evaluating Proliferation and Differentiation Markers in Developing Brunner's Glands. [<https://scholarsbank.uoregon.edu/xmlui/handle/1794/22869>].
- Noah TK, Kazanjian A, Whitsett J, Shroyer NF. SAM Pointed Domain ETS Factor (SPDEF) regulates terminal differentiation and maturation of intestinal goblet cells. *Exp Cell Res* 316 (3): 452-465.
- Obuoforibo AA, Martin BF. 1977. Postnatal growth of Brunner's glands in the mouse. *J. Anat* 124: 779–790.
- Parappilly M. 2016. Insights into the Development of Gastrointestinal Brunner's Gland: Critical Stem Cells and Differentiation Factors. <https://scholarsbank.uoregon.edu/xmlui/handle/1794/20348>.
- Specian RD, Oliver MG. 1991. Functional biology of intestinal goblet cells. *Am. J. Physiol.* 260: C183-93.

- Wang M-C, Li C-L, Cui J, Jiao M, Wu T, Jing LI, Nan K-J. 2015. BMI-1, a promising therapeutic target for human cancer. *Oncol. Lett.* 10:583–588.
- Wang Y, Srinivasan K, Siddiqui MR, George SP, Tomar A, Khurana S. 2008. A novel role for villin in intestinal epithelial cell survival and homeostasis. *J. Biol. Chem.* 283: 9454–64.
- Wood LD, Montgomery EA. 2014. *Gastrointestinal Anatomy and Physiology: The Essentials*. Oxford: John Wiley & Sons, Ltd.
- Wroblewski LE, Peek RM, Wilson KT. 2010. *Helicobacter pylori and Gastric Cancer: Factors That Modulate Disease Risk*. *Clin. Microbiol. Rev.* 23:713–739.